Proceedings of the 11th ICPMG 2026
11th International Conference on Physical Modelling in Geotechnics
8-12 June 2026, Zurich, Switzerland

An educational approach to soil dynamics: small-scale centrifuge modelling of resonance, pore pressure, and wave propagation

D. Cubides
Universidad de los Andes, Bogotá, Colombia, d.cubidesr@uniandes.edu.co

B. Caicedo
Universidad de los Andes, Bogotá, Colombia, bcaicedo@uniandes.edu.co

ABSTRACT: Soil liquefaction has been extensively studied worldwide through centrifuge modelling and large-scale experiments. However, micro-scale laminar box devices coupled with geotechnical centrifuges provide an innovative opportunity not only for research but also for education in soil dynamics. This study presents an experimental program conducted at Universidad de los Andes (Colombia), where a uniquely compact centrifuge-shaking system with a very small laminar box was implemented to reproduce pore pressure generation and wave propagation in sandy soils under unidirectional seismic loading. The setup, combining a micro-laminar box, latex membranes, pore pressure sensors, and accelerometers, enabled the direct observation of fundamental soil dynamics phenomena such as resonance, pore pressure build-up, and wave amplification. By scaling pore fluid viscosity with calibrated Brookfield viscometers, together with adjustments in drainage and confinement conditions, the experiments achieved results consistent with theoretical expectations. Measurable pore pressure build-up, clear identification of soil resonance frequency, and the visualization of wave transmission and amplification were obtained within the very small laminar box model, demonstrating the robustness of the methodology despite scale limitations. The primary contribution of this work is its educational approach: the compact centrifuge-shaking system serves as a didactic platform where complex soil–fluid–structure interactions can be physically observed at reduced scale.

1 INTRODUCTION

Soil liquefaction and related soil–structure interaction phenomena remain major challenges in geotechnical earthquake engineering. Classical approaches for studying these processes rely on empirical correlations, element tests, and numerical simulations. Although these methods have proven valuable, they often fail to capture the coupled and transient nature of pore pressure generation, resonance, and wave propagation in granular soils under cyclic loading (Seed & Idriss, 1971; Kramer, 1996).

Physical modelling in geotechnical centrifuges has provided an essential link between theory and field behaviour by reproducing stress similitude at reduced scale (Taylor, 1995). However, most centrifuge experiments are designed primarily for research, using large laminar boxes and complex shaking systems that limit accessibility and direct visualization.

This study introduces a compact centrifuge–shaker system developed to illustrate soil dynamics phenomena such as resonance, pore pressure build-up, and wave amplification within a micro-scale laminar box. The configuration combines a simplified boundary system, direct instrumentation, and viscosity-scaled fluids to reproduce undrained and drained responses under seismic excitation.

The main objective of this paper is twofold: (i) to document the development of this micro-scale centrifuge-based experimental platform at Universidad de los Andes (Colombia), and (ii) to demonstrate its educational value as a didactic tool that bridges theoretical soil dynamics concepts with observable laboratory behaviour.

2 EXPERIMENTAL SETUP

The experimental program was conducted in the geotechnical centrifuge facility at Universidad de los Andes (Colombia). The tests were designed to reproduce one-dimensional shear wave propagation and pore pressure generation under controlled seismic excitation. The following sections describe the configuration of the physical model, the instrumentation employed, and the test procedure.

2.1 Equipment and instrumentation

The testing equipment consisted of a micro-scale laminar box mounted on the arm of the geotechnical centrifuge (Chaparro et al., 2022) and a compact piezoelectric shaking system used to generate horizontal shear motion.

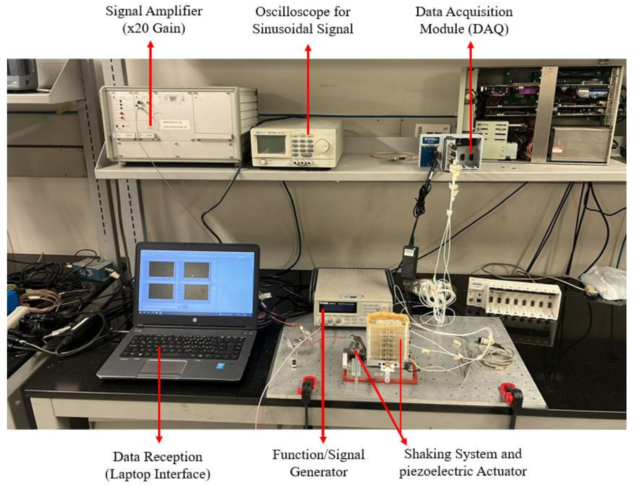

Figure 1. Experimental setup for the sinusoidal excitation test.

The laminar box was built from lightweight aluminium frames separated by low-friction polymer sheets to allow free shear deformation during excitation.

The shaking system included a piezoelectric actuator controlled by a signal generator and amplifier, providing precise control of input amplitude and frequency. Frequency sweep tests were performed to identify the resonance of the soil column, while fixed-frequency sinusoidal excitations were used to simulate unidirectional seismic loading.

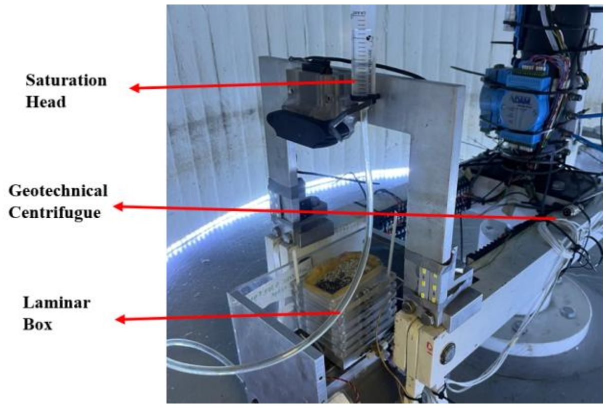

Figure 2. Assembly of the laminar box in the geotechnical centrifuge and sample saturation head

The instrumentation comprised three accelerometers located at the base, mid-depth, and surface of the deposit, and a pore pressure transducer installed at the base. The sensors were calibrated before testing to ensure consistent readings. Data acquisition was performed through a high-speed logger synchronized with the excitation signal, allowing direct comparison between input and response.

2.2 Materials and model preparation

The granular material used was Guamo sand, a well-characterized soil in Colombian geotechnical practice (Ruge et al., 2024). Its physical properties (specific gravity, maximum and minimum void ratios) made it suitable for studying liquefaction susceptibility (Jiménez, 2011). To replicate loose deposit conditions, sample density was controlled by pluviation methods. Two approaches were demonstrated to highlight their effect: (i) dry pluviation with negligible drop height, and (ii) pluviation over a thin water–glycerin layer.

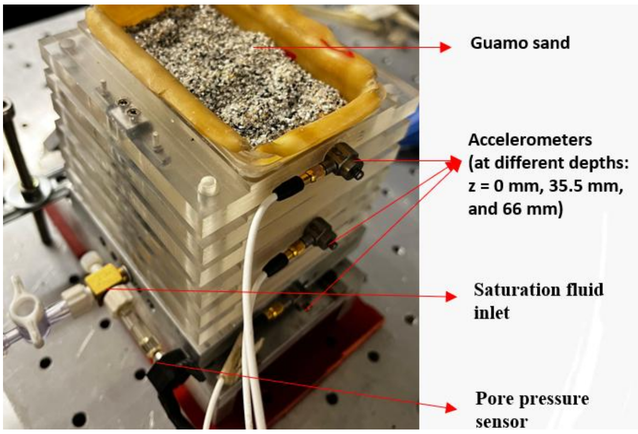

Figure 3. Instrumentation of the micro-scale laminar box model.

The second method proved especially effective in achieving reproducible loose states and served as a valuable educational example of how sample preparation influences soil fabric and subsequent dynamic response. In certain configurations, small amounts of kaolin fines (~8%) were or thin surface layers of kaolin or vinyl were placed atop the deposit to illustrate controlled drainage and confinement effects.

2.3 Sample preparation and saturation methodology

The preparation of the sand deposit was a critical stage of the experimental program, as it determined the initial density and uniformity of the model. Two pluviation methods were employed to control the relative density of the soil: dry pluviation and pluviation over a thin water layer.

In the dry pluviation method, the sand was allowed to fall freely through a funnel with a fixed opening and minimal drop height to reduce particle momentum and segregation. This approach produced moderately loose deposits, suitable for comparison with more controlled conditions.

Among the preparation methods, pluviation over a water film proved most effective for achieving uniformly loose deposits. The presence of a thin water layer at the base reduced particle settling velocity, allowing more random rearrangement and a looser structure. When the pore fluid consisted of water–glycerin mixtures, the increased viscosity further slowed sedimentation in accordance with Stokes' law (Stokes, 1851), promoting greater uniformity. This preparation method produced the most critical undrained response within the experimental programme reaching a maximum hydrostatic-reference excess pore pressure ratio of Ru,h=0.63. Although this does not represent full liquefaction, it indicates a significant reduction in effective stress relative to the theoretical hydrostatic state. Considering the small dimensions of the micro-scale model and the inherent scale constraints, achieving this level of pore pressure build-up represents a significant experimental result and demonstrates the capability of the system to reproduce near-liquefaction conditions.

After deposition, the samples were saturated using a low hydraulic head, following a controlled upward flow procedure. A constant head reservoir supplied the fluid from the base of the laminar box, maintaining a gentle and uniform percolation front. This slow infiltration minimized air entrapment and promoted complete saturation, ensuring stable pore pressure measurements during dynamic loading. The use of a low-pressure head also allowed students to visually follow the gradual wetting of the deposit, reinforcing theoretical concepts such as hydraulic conductivity, air dissolution, and effective saturation in granular soils.

This combined procedure—controlled pluviation and low-head saturation—ensured repeatable initial conditions and consistent hydraulic response across tests, highlighting the influence of density, saturation, and fluid viscosity on the dynamic behaviour of the soil under cyclic loading in centrifuge modelling.

2.4 Membranes and containment

Latex membranes were manually fabricated by successive dipping of wooden molds into liquid latex. This simple process provided an elastic yet resistant barrier, containing the soil without overly constraining wave transmission.

2.5 Pore fluid viscosity scaling

One of the challenges in centrifuge modelling of saturated soils is reproducing prototype-scale hydraulic transients. To achieve realistic pore pressure evolution, the viscosity of the pore fluid was scaled according to the operating g-level using water–glycerin mixtures. These mixtures were calibrated at 23 ± 0.5 °C using a Brookfield rotational viscometer model DV-E (Brookfield Engineering, 2000). The calibration followed the manufacturer's torque stability criteria to ensure reliable measurements within the recommended shear rate range.

The resulting μ–composition curve showed the expected non-linear increase in viscosity with glycerin concentration. This relationship allowed the selection of a suitable mixture for each g-level, ensuring that the characteristic hydraulic diffusion time and pore pressure dissipation were consistent with similitude laws. The chosen mixtures provided a balance between experimental practicality and adherence to theoretical scaling, thereby improving the accuracy of pore pressure generation and dissipation during flight and shaking.

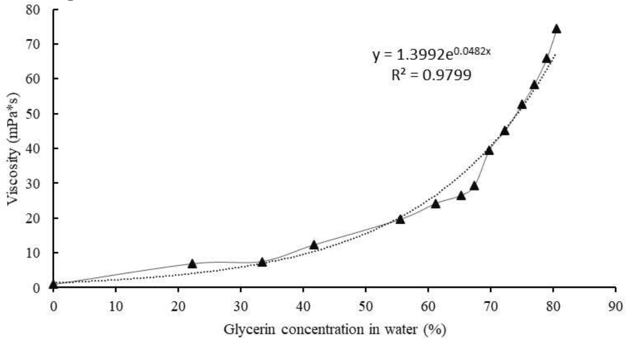

Figure 4. Relationship between glycerin concentration in water and viscosity.

Table 1 summarizes the adopted viscosity scaling scheme, showing the relationship between the applied gravity level, glycerin concentration, and resulting dynamic viscosity. The selected fluid at 60 g reached approximately 56 mPa·s, which was found to produce the most consistent pore pressure build-up and response times across tests.

Table 1. Summary of viscosity calibration for water–glycerin mixtures at 23 °C.

Gravity (N)	Glycerin in water 23 °C (%)	Viscosity (mPa·s)
20	64.88	18.2
30	69.00	25.3
40	73.30	42.5
50	75.14	50.0
60	76.58	56.1
70	79.58	65.45
80	82.55	74.8

From an educational standpoint, this calibration procedure allows students to directly connect a simple laboratory test—viscosity measurement—to the abstract concept of similitude in dynamic modelling.

3 RESULTS AND EDUCATIONAL EXAMPLES

3.1 Frequency sweep and resonance identification

To determine the natural frequency of the soil deposit, sinusoidal frequency sweeps were performed under centrifuge flight conditions using the piezoelectric shaker. Each test covered frequencies between 80 and 180 Hz at model scale, equivalent to approximately 1.3–3 Hz at prototype scale for 60 g.

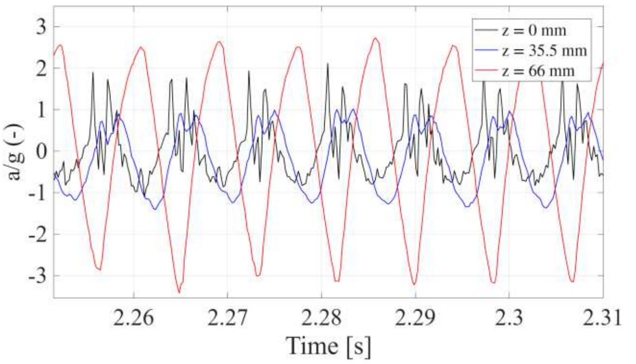

Figure 5. Sinusoidal signal recorded by the accelerometers at different depths (z = 0, 35.5 and 66 mm).

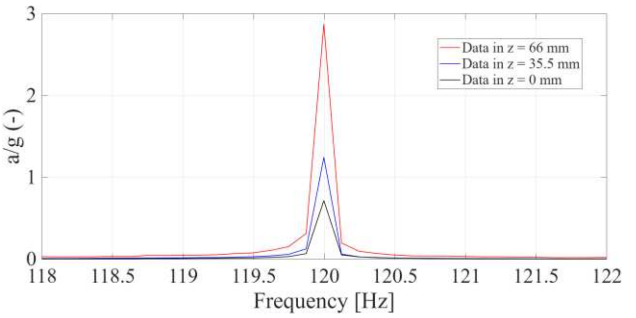

Figure 6. Fourier spectra at base, mid-depth, and surface.

As an example, Figure 5 shows the sinusoidal input signal generated at the base and recorded by accelerometers at different depths, while Figure 6 presents its Fourier spectrum at 120 Hz, corresponding to the model-scale excitation.

The amplification ratio, defined as $A = amax/amin$, was used to evaluate the dynamic response along the depth of the deposit. Figure 7 presents the amplification curve obtained from these tests, where a distinct peak at 120 Hz (≈ 2 Hz at prototype scale) confirms the resonance condition of the model (Kramer, 1996).

An independent estimate of the fundamental frequency was obtained using the quarter-wavelength approximation $f1 = Vs/(4H)$ (Kramer, 1996). With a model height of Hm=66mm and N=60, the corresponding prototype thickness is Hp=3.96m. The effective vertical stress in the deposit during centrifuge flight was approximately $\sigma v' \approx 55$–60kPa.

For loose saturated sands under this stress level, small-strain shear wave velocities in the range of 30–35 m/s are consistent with established correlations (Hardin and Richart, 1963; Kramer, 1996). Using a representative value of Vs=32m/s, the estimated fundamental frequency is:

$$f_1 = \frac{32m/s}{4 \cdot 3.96m} = 2.02Hz \quad (1)$$

which agrees closely with the experimentally observed resonance near 2 Hz.

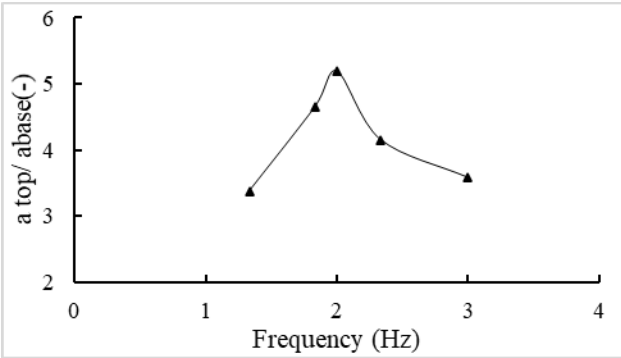

Figure 7. Amplification ratio (A = amax / amin) versus input frequency at model and prototype scales.

The main results of the frequency sweep are summarized in Table 2, including input frequency, base and surface accelerations, and corresponding amplification ratios. The prototype frequencies were computed using the similitude relationship:

$$Fr = \frac{F_m}{N} \quad (2)$$

where Fm (Hz) is the model input frequency, the centrifuge acceleration (g), and Fr (Hz) the equivalent prototype frequency.

Table 2. Summary of frequency sweep results and prototype scaling.

Frequency (Hz)	amax/amin	Fm/N (Hz)
80	3.4	1.33
110	4.7	1.83
120	5.2	2.00
140	4.2	2.33
180	3.6	3.00

3.2 Pore pressure generation

Both the water-only and water–glycerin tests were prepared using the same low-head saturation procedure to ensure comparable initial conditions. The relative density of the samples was controlled through gravimetric measurements of mass and volume, achieving Dr=20.7%, representative of a loose state. This preparation approach ensured consistent hydraulic and mechanical boundary conditions, isolating the influence of fluid viscosity on pore pressure response.

Table 3. Initial stress state at the transducer depth (N = 60, H = 66 mm)

Fluid, Condition	γ sat (kN/m³)	σv0 (kPa)	uh (kPa)	σ′v0 (kPa)
Water	19.4	77.12	39.00	27.77
Mix-Dry	18.5	73.54	40.96	14.64
Mix-Wet	18.3	72.65	40.96	14.09
Mix- kaolin and vinyl- dry	16.6	66.04	40.96	20.31

During centrifuge spin-up, pore pressure increased progressively as the acceleration level approached N=60. Importantly, even after reaching the target g-level, the recorded pore pressure continued to rise gradually prior to the application of cyclic loading. This behaviour is attributed to the small model scale, evolving hydraulic gradients, and ongoing particle rearrangement under sustained centrifugal acceleration. As a result, a strictly stabilized hydrostatic plateau was not achieved before excitation.

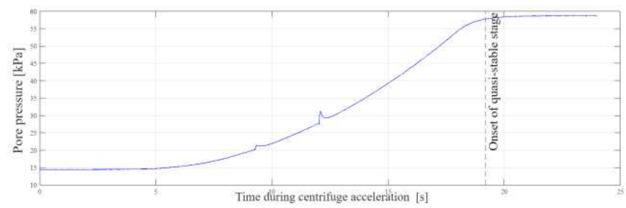

Figure 8. Example of pore pressure evolution during centrifuge spin-up prior to excitation.

Figure 8 illustrates an example of pore pressure evolution during centrifuge spin-up. As shown, pore pressure increases progressively as the g-level approaches 60 and does not reach a strictly horizontal stabilization plateau before excitation. Small transient peaks are observed during acceleration stages, likely associated with minor inertial perturbations and hydraulic redistribution within the deposit.

For this reason, pore pressure response is interpreted using two complementary reference baselines.

The theoretical hydrostatic pressure is defined as:

$$u_h = N\gamma_f H_m \quad (3)$$

where N is the centrifuge acceleration level, γf is the unit weight of the pore fluid, and Hm is the model height. This value represents the ideal fluid contribution under centrifuge similitude and provides a physically consistent benchmark for interpreting flight-induced pore pressure evolution.

The measured pore pressure immediately before excitation, denoted as u_0, reflects the actual in-flight stress condition at the onset of shaking. Because the baseline was still evolving prior to excitation, the theoretical hydrostatic reference plays a fundamental role in distinguishing spin-up effects from cyclically induced pore pressure increments.

Accordingly, two excess pore pressure ratios are reported:

Hydrostatic-reference ratio:

$$R_{u,h} = \frac{u_{max} - u_h}{\sigma_{v0} - u_h} \quad (4)$$

which provides a physically consistent benchmark under ideal similitude conditions and is particularly relevant for the didactic interpretation of flight-induced pore pressure evolution. Second, an incremental ratio referenced to the measured pore pressure immediately before excitation u_0 is also reported:

$$R_{u,0} = \frac{u_{max} - u_0}{\sigma_{v0} - u_0} \quad (5)$$

Figures 9 and 10 present the base acceleration and corresponding pore pressure response for the water and water–glycerin configurations at 120 Hz. The water-only test exhibited negligible pore pressure increment during excitation, consistent with drained behaviour. In contrast, the glycerin mixture produced measurable pore pressure build-up.

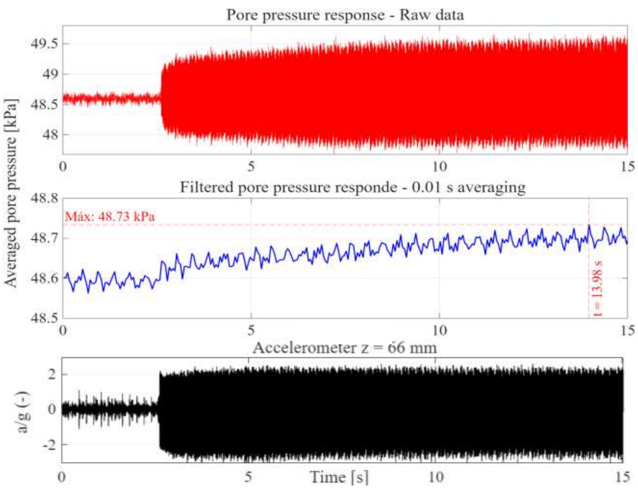

Figure 9. Pore pressure response of the soil at 120 Hz excitation with water.

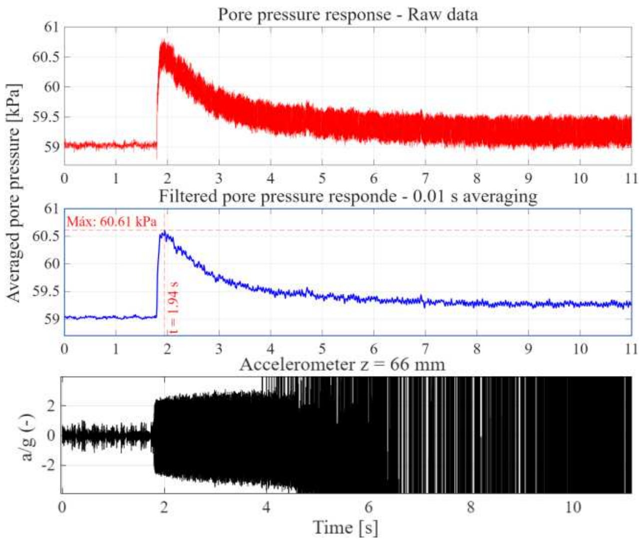

Figure 10. Pore pressure response of the soil at 120 Hz excitation with water–glycerin mixture.

When the viscous mixture was combined with pluviation over a thin water–glycerin layer (Figure 11), a looser and more homogeneous deposit was obtained. In this configuration, pore pressure increased rapidly during excitation, reaching Δu=2.29kPa. Using the hydrostatic reference, this corresponds to Ru,h=0.63, whereas the incremental ratio referenced to the measured pre-excitation baseline yields $Ru,0$=0.039.

Similarly, the partially confined configuration shown in Figure 12 produced Δu=3.94 kPa, resulting in Ru,h=0.35 and $Ru,0$=0.194.

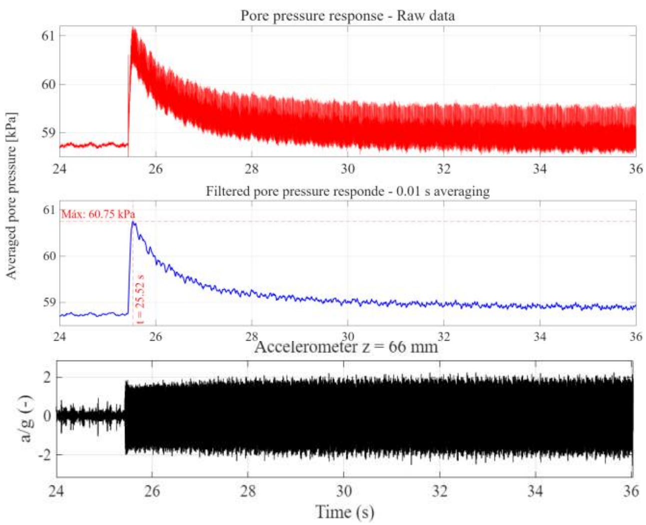

Figure 11. Pore pressure response for the test prepared by pluviation over a thin water layer, showing the highest hydrostatic-reference excess pore pressure ratio (Ru,h = 0.63) obtained at loose density.

These results demonstrate that while the cyclically induced pore pressure increments remain moderate in absolute magnitude, the comparison between Ru,h and $Ru,0$ highlights the contribution of flight-induced pore pressure evolution relative to dynamic excitation. This distinction is particularly relevant in micro-scale centrifuge modelling, where spin-up effects and hydraulic equilibration may significantly influence the pre-excitation stress state.

All cyclic excitation tests presented in this section were performed at 120 Hz model frequency with a constant input amplitude of 1 V at the signal generator.

3.3 Influence of drainage restrictions and boundary conditions

The influence of drainage and boundary confinement was evaluated through tests involving variations in surface sealing and fines content. In particular, one test was performed with a sand–kaolin mixture containing 8 % kaolin by dry weight and a vinyl film placed over the surface to simulate a low-permeability layer preventing upward drainage.

In this configuration, the initial response of the model showed a greater difference between the stabilized pressure and the maximum recorded pore pressure, resulting in Δu=3.94 kPa (increment referenced to u_0), with Ru,h=0.35 and Ru,0=0.194. This behaviour suggests that the addition of a small percentage of cohesive fines promotes the build-up of pore pressure by reducing permeability and facilitating localized undrained conditions. Figure 12 shows the time history of pore pressure for this test compared with the clean-sand configuration.

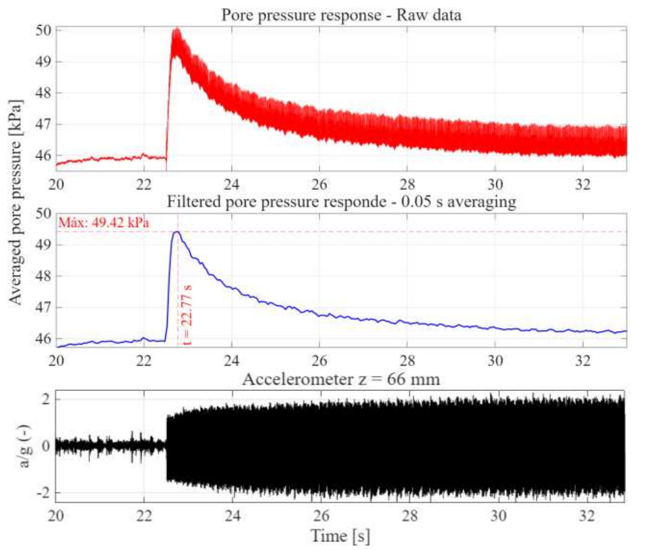

Figure 12. Pore pressure response under partially confined drainage conditions.

Compared with the pure-sand model, which began to generate slight pore pressure increases during centrifuge spin-up, the kaolin-enriched sample maintained a more stable initial condition and developed pressure build-up primarily during cyclic loading. This indicates that fine material addition helps preserve the prepared state of the model during spin-up, enhancing experimental control and reproducibility.

From an educational standpoint, this test illustrates how minor variations in fines content and drainage boundaries influence the hydraulic and mechanical response of granular soils under dynamic loading. It reinforces key soil dynamics principles such as permeability control, undrained response, and pore pressure generation, providing a clear and observable example for classroom and laboratory teaching.

3.4 Summary of Main Centrifuge Tests and Pore Pressure Response Parameters

To consolidate the experimental observations, the main centrifuge tests were summarized in Table 4. This table includes the key parameters describing the pore pressure behaviour for each configuration: the type of fluid used, the pluviation method, the stabilized and maximum pore pressures, the pressure difference (ΔP), the maximum excess pore pressure ratio (Ru), the number of loading cycles, and the presence or absence of confining layers.

Table 4. Pore pressure increments and excess pore pressure ratios.

Fluid, Condition	**u_0 (kPa)**	**umax (kPa)**	**Δu (kPa)**	**Ru,h**	**Ru,0**
Water	49.35	49.47	0.12	0.275	0.004
Mix-Dry	58.90	60.58	1.68	0.602	0.115
Mix-Wet	58.56	60.85	2.29	0.628	0.162
Mix-kaolin and Vinyl- Dry	45.73	49.67	3.94	0.347	0.194

The summarized results clearly highlight the progressive increase in ΔP and Ru,0 with the introduction of viscous fluids and partial drainage restrictions. While the pure-sand and water-saturated configuration remained fully drained, the addition of glycerin and kaolin produced conditions closer to undrained behaviour, leading to higher pore pressure ratios and delayed dissipation (Kramer, 1996; Taylor, 1995).

From an educational perspective, this summary enables students to identify the link between fluid viscosity, boundary permeability, and excess pore pressure response using a compact comparative dataset. It also serves as a bridge to the following section, where the evolution of soil behaviour through repeated tests and progressive densification is discussed.

3.5 Progressive densification and data interpretation

During the centrifuge flight, the soil deposit exhibited a gradual increase in density as a result of both the sustained centrifugal acceleration and the cyclic sinusoidal excitation applied during testing. This progressive densification led to subtle changes in the dynamic response of the model, observable through variations in amplitude and resonance behaviour over time.

As the tests progressed, the amplitude of the measured acceleration waves became progressively larger, reflecting a stiffer and more stable soil structure capable of transmitting greater shear stresses. This phenomenon indicates that cyclic excitation at the model scale produces continuous rearrangement of particles, consistent with vibration-induced compaction observed in granular materials (Terzaghi et al., 1996).

The resonance of the soil deposit, identified near 2 Hz (prototype scale), played a key role in the observed pore pressure build-up. At frequencies close to resonance, the dynamic response was amplified, leading to higher excess pore pressure ratios (Kramer, 1996).

4 CONCLUSIONS

This study presented a comprehensive experimental program conducted using a micro-scale centrifuge–shaker system developed to reproduce and visualize the fundamental mechanisms of soil dynamics, including resonance, pore pressure build-up, and wave propagation. The results confirmed that this configuration not only allows the correct physical reproduction of these processes but also provides a didactic platform through which complex soil–fluid–structure interactions can be observed and understood at reduced scale.

The identification of soil resonance during frequency sweep tests demonstrated that the centrifuge system can accurately reproduce the dynamic amplification phenomena expected for granular deposits. A clear resonance peak was identified near 2 Hz at prototype scale, matching theoretical estimations. The ability to observe this amplification directly at the surface of the model enables students to connect theoretical frequency–response functions with a real, measurable phenomenon, transforming resonance from an abstract concept into an observable dynamic event.

The analysis of pore pressure generation confirmed the significance of viscosity scaling in modifying drainage conditions within the micro-scale centrifuge model. While excess pore pressure ratios referenced to the measured pre-excitation baseline remained below Ru,0=0.2, hydrostatic-reference ratios reached values up to Ru,h=0.63. This distinction highlights the importance of separating flight-induced pore pressure evolution from cyclically generated increments when interpreting centrifuge data at small scale.

The incorporation of 8 % kaolin and the use of a vinyl surface layer introduced partial drainage restrictions that modified the hydraulic boundary conditions of the model. The difference between stabilized and peak pressures was greater, highlighting how cohesive fines and limited permeability influence pore pressure development. This configuration preserved the stability of the initial state during flight and emphasized the influence of permeability and boundary confinement on dynamic soil response, offering a clear example for classroom discussion.

Progressive densification was observed as the tests were repeated, evidenced by a gradual increase in stiffness and a corresponding rise in resonance frequency—from approximately 2.0 to 2.3 Hz at prototype scale—together with lower Ru,0 values. This evolution of the soil fabric can be easily recognized in the recorded acceleration and pore pressure data, providing a concrete means of linking laboratory measurements to field-scale phenomena such as vibration-induced compaction and stiffness recovery.

Overall, the results of this work highlight the educational value of the small-scale centrifuge platform. Its simplicity, reproducibility, and visible response allow for the direct integration of physical modelling into teaching practices. The system bridges the gap between theoretical instruction and experimental observation, offering an accessible way to demonstrate essential principles of soil dynamics, resonance, wave propagation, and liquefaction-related pore pressure response. Beyond its technical achievements, the present study underscores that micro-centrifuge modelling can serve not only as a research tool but also as a pedagogical instrument that fosters active learning and a deeper understanding of geotechnical earthquake engineering.

REFERENCES

Brookfield Engineering (2000). More solutions to sticky problems: A guide to getting more from your Brookfield Viscometer. Brookfield Engineering Laboratories, Middleboro, MA.

Chaparro, J., Jara, A., Cabrera, M. & Caicedo, B. (2022). A micro laminar box coupled with a piezoelectric shaking table for centrifuge. Ingeniería e Investigación, 19(September).

Hardin, B.O., & Richart, F.E. (1963). Elastic wave velocities in granular soils. Journal of the Soil Mechanics and Foundations Division, ASCE, 89(SM1), 33–65.

Jiménez, O.J. (2011). Análisis del comportamiento de licuación por flujo en la arena del Guamo. Undergraduate thesis, Universidad de los Andes, Bogotá, Colombia.

Kramer, S.L. (1996). Geotechnical earthquake engineering. Prentice Hall, Upper Saddle River, NJ.

Ruge, J.C., Molina-Gómez, F., Olarte, M.C., Camacho-Tauta, J., Reyes-Ortiz, Ó., Larrahondo, J.M., Vacca, H.A., Prada, L.F., Ramos-Cañón, A., Alvarado, Y.A., Reyes, F.J., Cabrera, M.A., Caicedo-Hormaza, B., Naranjo, J.S., Otálvaro, I.F., Gómez-Jiménez, A., Galvis, M.A., Carmona, J.E., García, C.A., … Rojas, J.P. (2024). Inter-laboratory testing program for the physical characterization of Guamo sand. Ingeniería e Investigación, 44(3), e113488. https://doi.org/10.15446/ing.investig.113488

Seed, H.B. & Idriss, I.M. (1971). Simplified procedure for evaluating soil liquefaction potential. Journal of the Soil Mechanics and Foundations Division, ASCE, 97(SM9), 1249–1273. https://doi.org/10.1061/JSFEAQ.0001662

Stokes, G.G. (1851). On the effect of the internal friction of fluids on the motion of pendulums. Transactions of the Cambridge Philosophical Society, 9, 8–106.

Taylor, R.N. (1995). Geotechnical centrifuge technology. Blackie Academic & Professional, Glasgow. https://doi.org/10.1201/9781482269321